

NANO · MICRO  
**small**

Supporting Information

for *Small*, DOI 10.1002/smll.202302581

Sodium Incorporation for Performance Improvement of Solution-Processed Submicron  
CuIn(S,Se)<sub>2</sub> Thin Film Solar Cells

*Yao Gao, Guanchao Yin\* and Martina Schmid\**

Supporting Information

**Sodium incorporation for performance improvement of solution-processed submicron  $\text{CuIn}(\text{S},\text{Se})_2$  thin film solar cells**

Yao Gao, Guanchao Yin\*, Martina Schmid\*

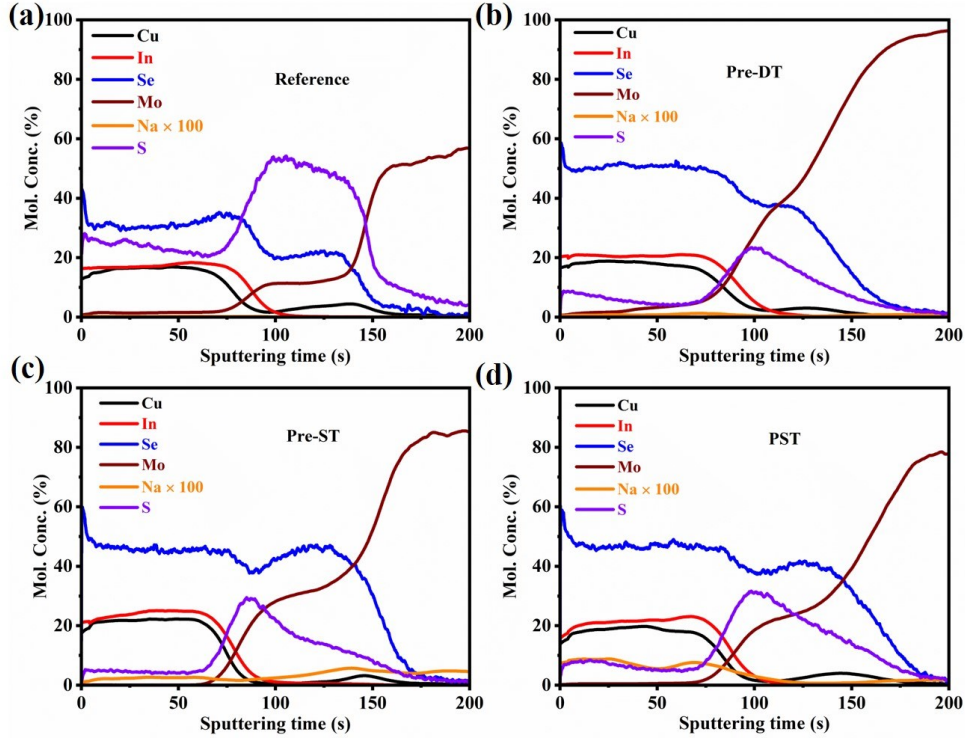


Figure S1 Composition depth profiles of CISSe absorbers without/with Na incorporation measured by GDOES. (a) Reference CISSe, (b) Pre-DT CISSe, (c) Pre-ST CISSe, and (d) PST CISSe. All these measurements are carried out after removing the CdS/i-ZnO/AZO top layers by 10% HCl etching.

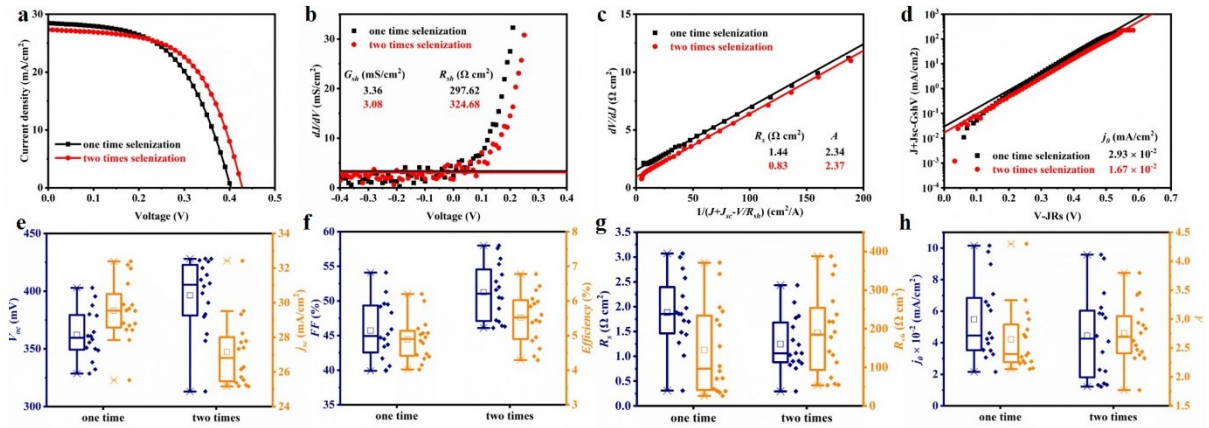


Figure S2 (a)  $J-V$  curves, (b) shunt resistance ( $R_{sh}$ ), (c) series resistance ( $R_s$ ) and ideality factor ( $A$ ), and (d) reverse saturation current density ( $j_0$ ) of best CISSe solar cells with one time or two times selenization. Statistical distributions of (e)  $V_{oc}$  and  $j_{sc}$ , (f)  $FF$  and Efficiency, (g)  $R_s$  and  $R_{sh}$ , (h)  $j_0$  and  $A$  derived from 16 devices for CISSe solar cells with one time or two times selenization.

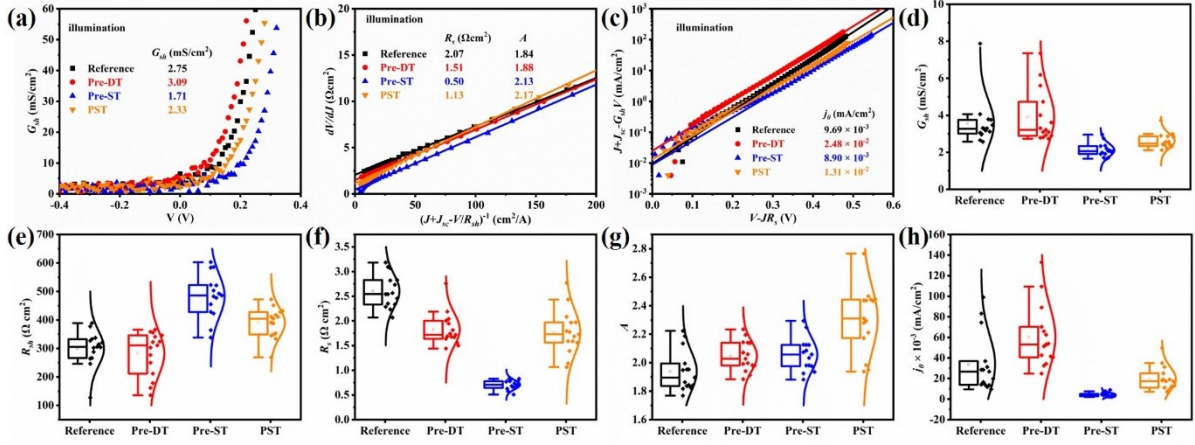


Figure S3 Plots of (a)  $G_{sh}$  vs.  $V$ , (b)  $dV/dJ$  vs.  $1/(J+J_{sc}-V/R_{sh})$  for derivation of  $R_s$  and  $A$ , and (c) semi-logarithmic plot of  $J+J_{sc}-G_{sh}V$  vs.  $V-JR_s$  to determine  $j_0$ . Statistical distribution of (d)  $G_{sh}$ , (e)  $R_{sh}$ , (f)  $R_s$ , (g)  $A$ , and (h)  $j_0$ .

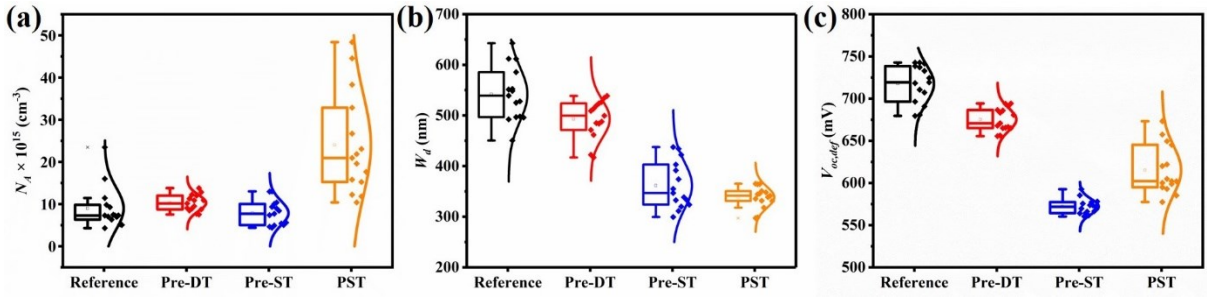


Figure S4 Statistical distribution of (a)  $N_A$ , (b)  $W_d$ , and (c)  $V_{oc,def}$  derived from measurements of 15 CISSe sub-cells.

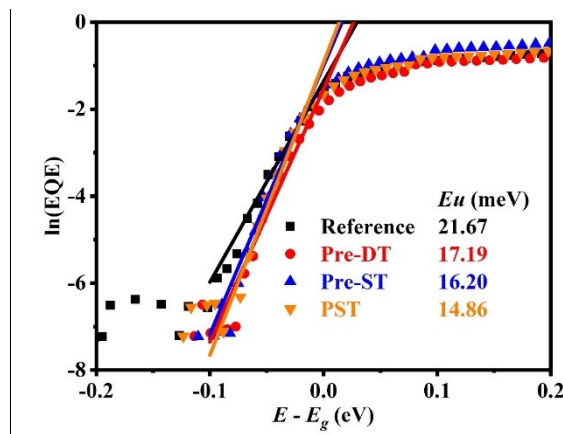


Figure S5  $\ln(\text{EQE})$  vs.  $(E - E_g)$  of CISSe solar cells in the long-wavelength edge of EQE for the calculation of  $E_U$  of CISSe absorbers with various Na incorporation strategies.

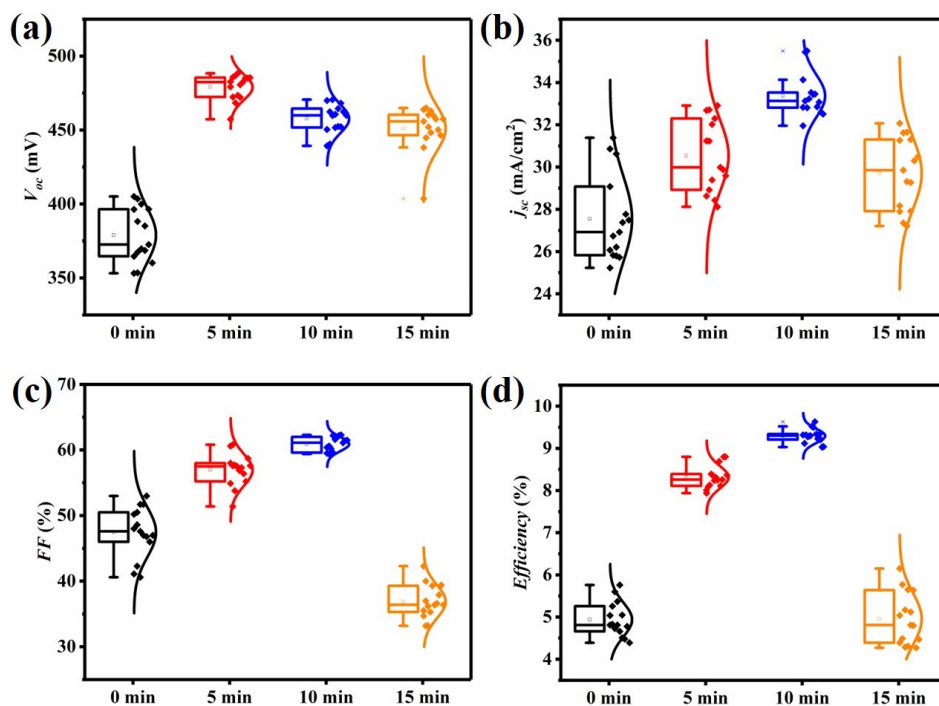


Figure S6 Statistical distribution of (a)  $V_{oc}$ , (b)  $j_{sc}$ , (c)  $FF$ , and (d) efficiency derived from 15 CISSe devices with 1 M NaCl aqueous-ethanol solution Pre-ST for various times.

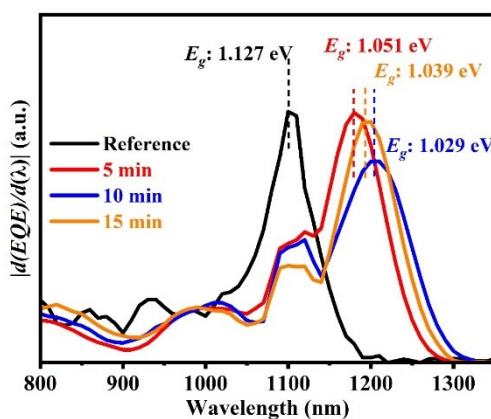


Figure S7 Band gaps of CISSe devices with 1 M NaCl aqueous-ethanol solution Pre-ST for various times.

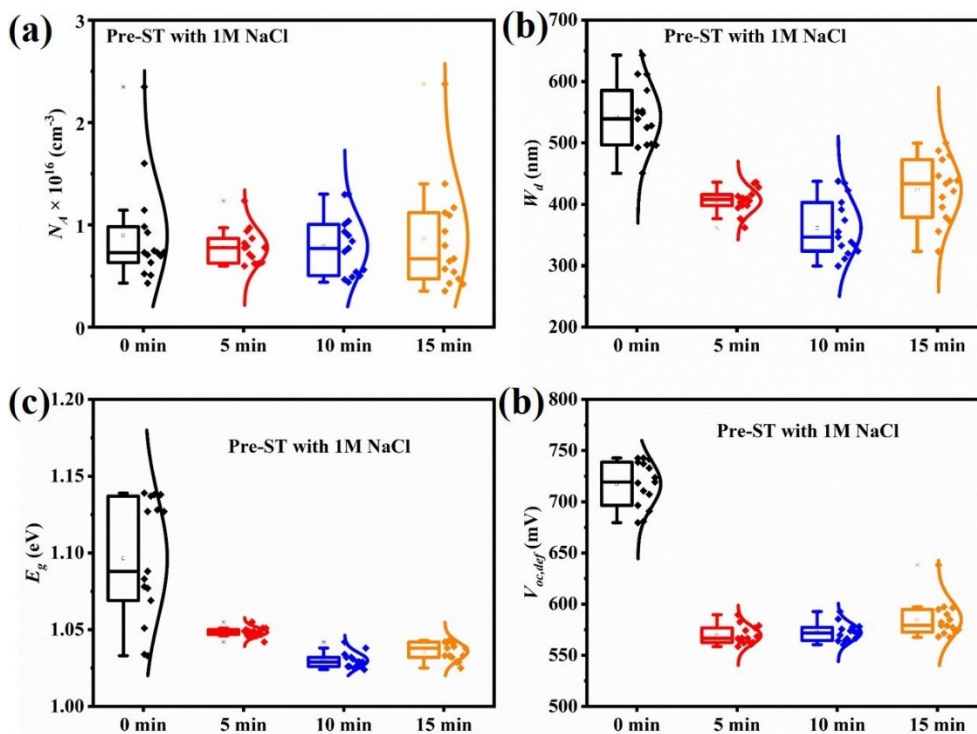


Figure S8 Statistical distribution of (a)  $N_A$ , (b)  $W_d$ , (c)  $E_g$ , and (d)  $V_{oc,def}$  derived from 15 CISSE devices with 1 M NaCl aqueous-ethanol solution Pre-ST for various times.

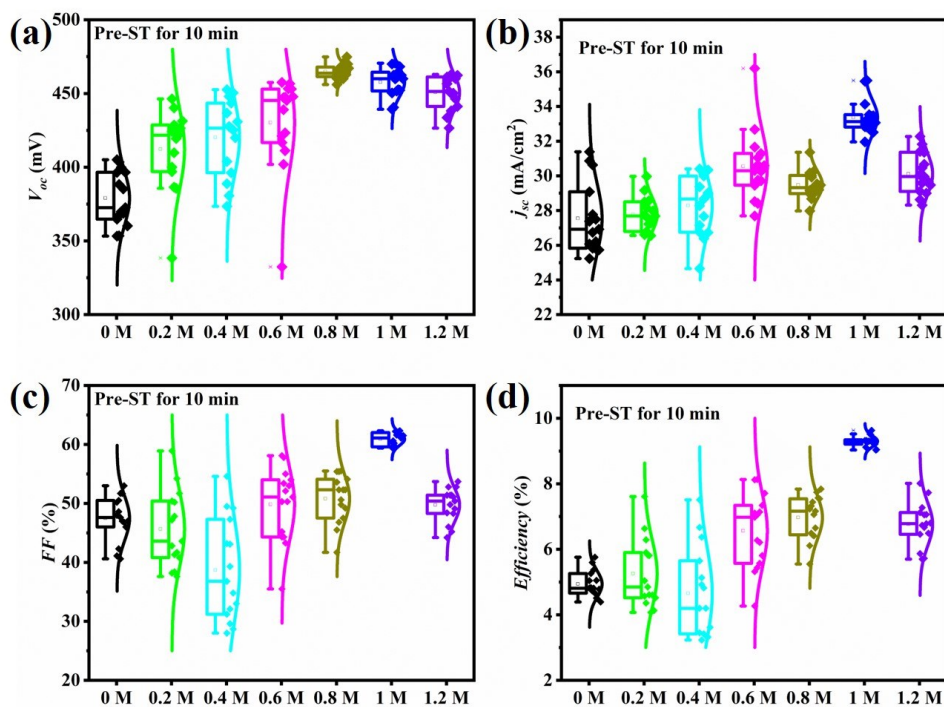


Figure S9 Statistical distribution of (a)  $V_{oc}$ , (b)  $j_{sc}$ , (c)  $FF$ , and (d) efficiency derived from 15 CISSE devices with Pre-ST for 10 min in various concentrations of NaCl aqueous-ethanol solution.



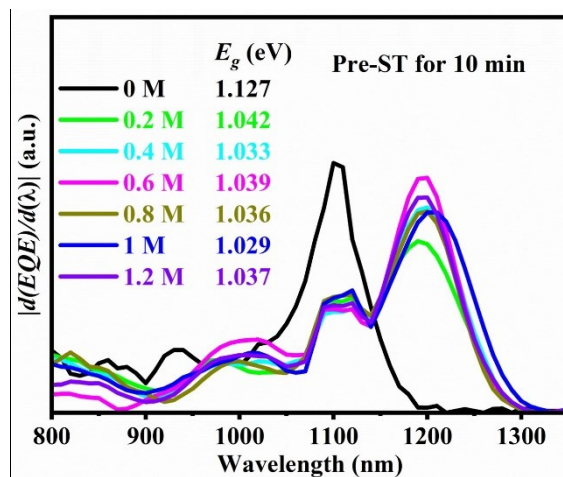


Figure S10 Band gaps of CISSe devices with Pre-ST for 10 min in various concentrations of NaCl aqueous-ethanol solution.

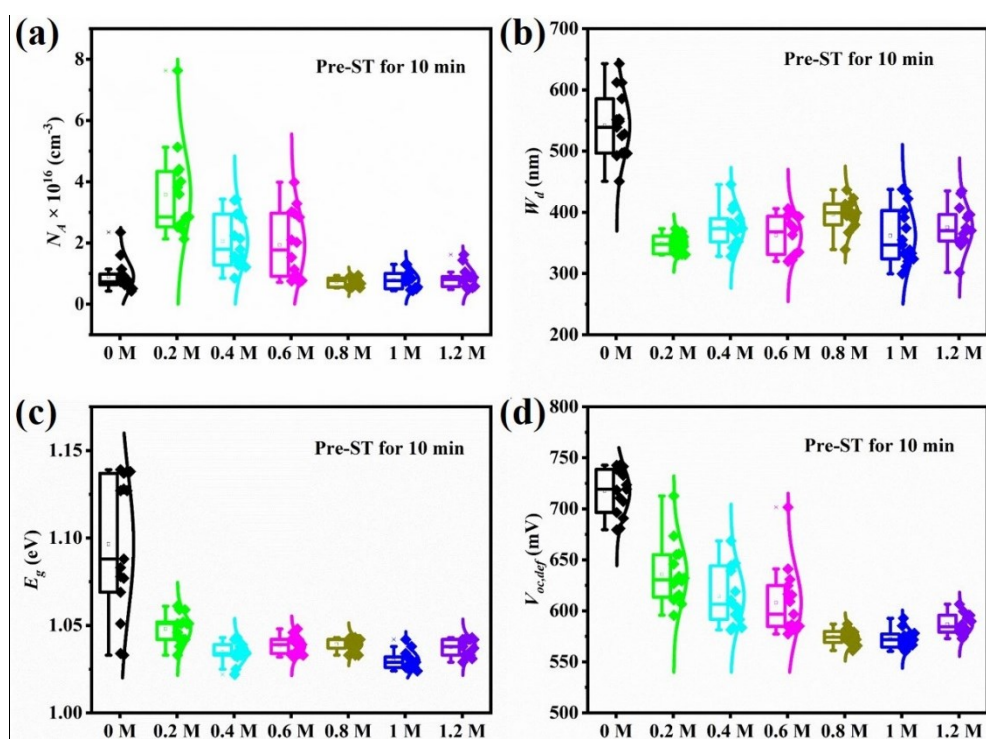


Figure S11 Statistical distribution of (a)  $N_A$ , (b)  $W_d$ , (c)  $E_g$ , and (d)  $V_{oc,def}$  derived from 15 CISSe devices with Pre-ST for 10 min in various concentrations of NaCl aqueous-ethanol solution.